Identification of a Partially Rate-Determining Step in the Catalytic Mechanism of cAMP-Dependent Protein Kinase: A Transient Kinetic Study Using Stopped-Flow Fluorescence Spectroscopy†

John Lew,‡ Susan S. Taylor,‡ and Joseph A. Adams*,§

Department of Chemistry, San Diego State University, San Diego, California 92182-1030, and Department of Chemistry and Biochemistry, University of California, San Diego, La Jolla, California 92093-0654

Received December 27, 1996; Revised Manuscript Received March 18, 1997⊗

ABSTRACT: The kinetics of nucleotide binding and phosphoryl group transfer were measured in the catalytic subunit of cAMP-dependent protein kinase using stopped-flow fluorescence spectroscopy and an acrylodan-labeled derivative of this enzyme, which we have previously shown to have kinetic properties similar to those for the wild-type enzyme (Lew et al., 1996). The fluorescence emission spectrum of this enzyme is quenched differentially by ATP and ADP so that both the binding of ligands and phosphoryl group transfer at the active site can be monitored selectively. The association and dissociation rate constants for both nucleotides were measured using two methods: relaxation and competition binding. The ratio of the observed dissociation and association rate constants by both methods are consistent with K_d measurements (25 μM) determined by equilibrium fluorescence quenching. The dissociation rate constant for ADP (100 s^{-1}) is approximately 2.5-fold larger than k_{cat} (39 s^{-1}). A full viscosity effect was measured for k_{cat}, suggesting that a diffusive step or steps limit maximum turnover. Pre-steady-state kinetic transients are biphasic and were fitted to observed rate constants of 500 s^{-1} and 60 s^{-1} at 500 μM Kemptide (LRRASLG). Metal substitution studies (Mg^{2+} vs Mn^{2+}) indicate that this first phase represents the phosphoryl group transfer step. Phosphopeptide release is faster than this second phase since the substrate is in rapid exchange with the enzyme and phosphorylation reduces the affinity of the peptide. The inability to assign this second phase to the chemical event or to product release implies that it reflects a viscosity-sensitive, protein conformational change that occurs after phosphoryl group transfer and prior to product release. Two conformational steps were detected in the binding of both ATP and ADP by relaxation methods that may be related to this second pre-steady-state kinetic phase. We suggest that this additional step in the kinetic mechanism may also occur in the wild-type enzyme and represents a large structural change in the enzyme during normal catalytic cycling.

Protein phosphorylation is a key regulatory theme in the control of nearly all pathways of mammalian signal transduction. The protein kinases, which catalyze these reactions, constitute the largest enzyme family known, with over 200 members presently identified (Hanks & Hunter, 1995). The considerable attention focused on this family of catalysts has stemmed from our knowledge of their essential role in cellular homeostasis, evidenced by an established link between aberrant forms of several kinases and oncogenesis and human disease. While the biological role of protein kinases has, in general, been extensively probed, our understanding of the relationship between their physiological function and catalytic mechanism at even a rudimentary level is poor. The one exception to this fact is the example of cAMP-dependent protein kinase (PKA),[1] by far the best understood member of this family at the physiological, structural, and mechanistic levels (Taylor et al., 1990). The early discovery of PKA was based on its central role in linking glycogen metabolism to β-adrenergic hormone signaling (Walsh et al., 1968). More recently, it has been recognized that this enzyme, in addition, is involved in the transcriptional regulation of gene expression (Montminy et al., 1990) as well as in cell cycle control (Frank & Greenberg, 1994; Grieco et al., 1996), emphasizing the diversity of cellular roles that this enzyme fulfills. In vivo, PKA exists as an inactive heterotetrameric holoenzyme, which undergoes activation in response to elevated cellular levels of cAMP, generating a regulatory subunit dimer (R_2) bound to four molecules of cAMP and two active catalytic subunits (C-subunit) according to the following mechanism (Taylor et al., 1990):

$$4\text{cAMP} + R_2C_2 \rightarrow R_2{\cdot}\text{cAMP}_4 + 2C$$

The X-ray crystal structure of the catalytic subunit of PKA has revealed that the catalytic core adopts a bilobal fold, the

† This work was supported by an NIH grant (GM54846), the California Metabolic Research Foundation, and the American Heart Association, California Affiliate (95-274), to J.A.A. and by an NIH grant (GM 19301) to S.S.T. J.L. is supported by a fellowship from the Medical Research Council of Canada.

* Author to whom correspondence should be addressed. Tel (619) 594-6196; fax (619) 594-1879; e-mail jadams@sundown.sdsu.edu.

‡ University of California, San Diego.

§ San Diego State University.

⊗ Abstract published in *Advance ACS Abstracts,* May 15, 1997.

[1] Abbreviations: Acr-PKA, mutant catalytic subunit (N326C) of cyclic AMP-dependent protein kinase labeled with acrylodan; C-subunit, catalytic subunit of cyclic AMP-dependent protein kinase; Kemptide, seven-residue peptide substrate LRRASLG; phosphokemptide, serine-phosphorylated Kemptide; PKA, cyclic AMP-dependent protein kinase; PKI, protein kinase inhibitor; R_2, regulatory subunit dimer.

S0006-2960(96)03164-9 CCC: $14.00

general structure of which is conserved among all protein kinases whose three-dimensional structures are known (Taylor & Radzio-Andzelm, 1994). The interface of the two lobes define an active-site cleft in which the adenosine moiety of ATP is deeply buried, the triphosphate group being directed toward the active-site cavity. At the mouth of the cleft is the binding site for peptide and protein substrates, and this is where phosphoryl group transfer occurs (Zheng et al., 1993a). The role of select key residues in catalysis can be inferred from the solved structure. Among several residues that are invariant among protein kinases, most are clustered around the active site. Lys-72, Lys-168, Gly-50, and Gly-52 stabilize the triphosphates of ATP, Asp-184 and Asn-171 are critical for metal binding, and Asp-166 has been proposed to function as a potential catalytic base (Madhusudan et al., 1994). In addition, the structures of several active vs inactive protein kinases has unveiled the role of conformational changes that are critical for enzyme function. In particular, an "activation loop" located at the mouth of the active site must be properly oriented in order to permit access of substrates to the active site (DeBont et al., 1993; Jeffrey et al., 1995). In many cases, this requires the activation loop to be phosphorylated on a conserved Ser or Thr residue (Thr-197 in PKA).

The kinetic mechanism for the phosphorylation of a synthetic peptide substrate, Kemptide, by PKA is viewed currently as a simple three-step process comprising substrate binding, phosphotransfer, and product release (Adams & Taylor, 1992; Grant & Adams, 1996). The steady-state kinetic mechanism is formally random but the preferred pathway is the initial binding of ATP followed by the addition of Kemptide, with the subsequent release of phosphokemptide and ADP at high Mg^{2+} concentrations (Cook et al., 1982; Kong & Cook, 1988; Whitehouse et al., 1983). The higher affinity of the enzyme for nucleotides, compared to that for substrate and product peptides, is consistent with this scheme (Whitehouse et al., 1983; Whitehouse & Walsh, 1983). Viscosity studies show that maximum turnover (k_{cat}) is controlled by a diffusive event, implying that the rate of phosphoryl group transfer is, at least, 10 times greater than that of product release (Adams & Taylor, 1992). The dissociation rate constant for Kemptide is large, which has led to the widely held assumption that the release of phosphokemptide does not limit k_{cat} and that the release of ADP is cleanly rate-limiting (Adams & Taylor, 1992). While viscosometric methods enable the partitioning of chemical and physical events, this technique could place only a lower limit on the rate of phosphoryl group transfer when applied to PKA (Adams & Taylor, 1992). Recently, however, rapid quenched-flow studies provided, for the first time, a rate value (500 s^{-1}) to be assigned to the phosphotransfer step (Grant & Adams, 1996). The rapid phosphoryl group transfer followed by the slow release of ADP accounts for the approximate 100-fold higher K_d for Kemptide than K_m.

Although pre-steady-state kinetic techniques have successfully identified the phosphoryl transfer step in PKA (Grant & Adams, 1996), the role of conformational changes and product release on maximum turnover is unclear. The inability to probe the internal enzyme mechanism in greater detail is attributed, in part, to the lack of appropriate biophysical probes. In particular, the intrinsic fluorescence emission signal from the enzyme is poor and has proven to be unsuitable as a monitor of substrate or product binding. To circumvent this problem, we have constructed several fluorescently tagged derivatives of PKA whose fluorescence emissions are sensitive to the binding of various ligands. One such derivative, labeled with acrylodan at position 326 in the C-terminal tail, is sensitive to the binding of nucleotides (Lew et al., 1996). This has permitted, for the first time, an investigation into the kinetics of nucleotide binding to the catalytic subunit of PKA using stopped-flow fluorescence spectroscopy. In this study, we report the identification of a novel conformational change which is partially rate-determining on k_{cat}. The role of conformational changes in catalysis has previously not been described for any protein kinase.

MATERIALS AND METHODS

Materials. Fluorescently labeled PKA (Acr-PKA) was generated and characterized as described in Lew et al. (1996). Peptides were synthesized at the Peptide and Oligonucleotide Facility at UCSD and were greater than 95% pure based on analysis by reverse-phase HPLC. Phosphokemptide was synthesized by complete turnover of Kemptide with C-subunit and purified by HPLC using a preparative C18 column according to previously published procedures (Qamar et al., 1992) . Nucleotides were purchased from Sigma. All other reagents, unless otherwise noted, were purchased from Fisher Scientific.

Steady-State Kinetic Assays. Kinetic analyses were obtained using a continuous spectrophotometric assay that couples ADP production with NADH oxidation catalyzed by pyruvate kinase and lactate dehydrogenase (Cook et al., 1982). The specific conditions of assay are given in Lew et al. (1996). Viscosometric measurements using sucrose as the viscosogenic agent were carried out and the data were interpreted according to Adams and Taylor (1992) The dissociation constant for phosphokemptide was determined by a product inhibition assay. Initial velocity vs Kemptide concentration in the absence or presence of varied, fixed concentrations of phosphokemptide was plotted and analyzed by assuming a functionally ordered bi-bi mechanism. Inhibition of the C-subunit by phosphokemptide was monitored by preequilibrating the enzyme with phosphokemptide and ATP (1 mM) before starting the reaction with Kemptide. All assays were conducted in buffer containing 20 mM MOPS, pH 7.0, 50 mM NaCl, and 10 mM $MgCl_2$ at 25 °C. The concentration of Acr-PKA was determined by titration of the enzyme activity with known amounts of the physiological inhibitor, PKI.

Transient Kinetic Assays. All transient kinetic measurements were made using an Applied Photophysics stopped-flow spectrometer fitted with a 420 nm cutoff filter between the cell and photomultiplier tube. The excitation wavelength was 380 nm and the bandpass was 4 nm. For data analysis, the average of 3−15 individual traces was used. All experiments were conducted under pseudo-first-order conditions defined by a ligand to enzyme concentration ratio at least 8:1. Rate constants and amplitudes were obtained by fitting of the data to equations describing a single- or double-exponential growth/decay using the Applied Photophysics software. Alternatively, the raw data was imported into the computer program KaleidaGraph (Synergy Software) and fit using similar equations. Fluorescence amplitude changes for exponential transients obtained from the stopped-flow instrument were corrected for an instrument dead time of 1.5 ms

Table 1: Steady-State Kinetic and Viscosity Parameters for Acr-PKA[a]

parameter	Acr-PKA	WT-PKA
k_{cat}[b] (s^{-1})	39 ± 2.1	26
K_{ATP}[b]	42 ± 4.7	17
$K_{Kemptide}$[b] (μM)	41 ± 3.4	25
$k_{cat}/K_{Kemptide}$[b] (μM^{-1} s^{-1})	0.94 ± 0.093	1.0
k_{cat}/K_{ATP}[b] (μM^{-1} s^{-1})	0.93 ± 0.16	1.5
$(k_{cat})^{\eta}$ [c]	1.2 ± 0.11	
$(k_{cat}/K_{Kemptide})^{\eta}$ [c]	0.13 ± 0.04	

[a] Measured under conditions described in Materials and Methods. [b] from Lew et al. (1996). [c] $(k_{cat})^{\eta}$ and $(k_{cat}/K_{Kemptide})^{\eta}$ are the slopes of $k_{cat}^{\circ}/k_{cat}$and $(k_{cat}/K_{Kemptide})^{\circ}/(k_{cat}/K_{Kemptide})$ vs η^{rel}, respectively, in Figure 1.

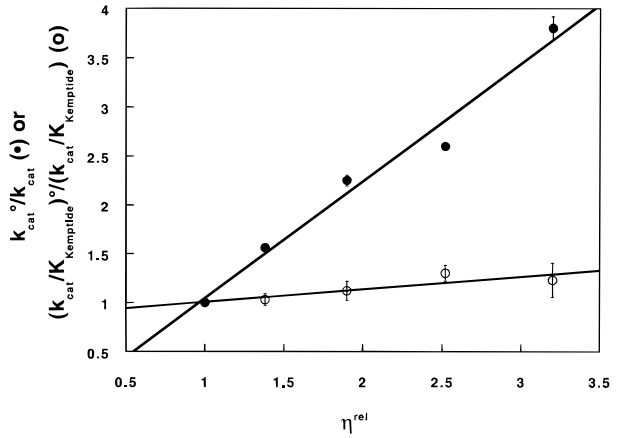

FIGURE 1: Effects of solvent viscosity on the steady-state kinetic parameters, k_{cat} and $k_{cat}/K_{Kemptide}$, for the phosphorylation of Kemptide by Acr-PKA. $(k_{cat})^{\circ}/k_{cat}$ (●) and $(k_{cat}/K_{Kemptide})^{\circ}/(k_{cat}/K_{Kemptide})$ (○) are the ratios of the observed steady-state kinetic parameters k_{cat} and $k_{cat}/K_{Kemptide}$ in the absence and presence of viscosogen.

when stated in the text, using the following equation:

$$\Delta F_c = \frac{\Delta F_{unc}}{\exp[-0.0015 k_{obs}]} \quad (1)$$

where ΔF_c and ΔF_{unc} are the corrected and uncorrected amplitudes obtained from the fitted data. Alternatively, the raw fluorescence data were imported in KaleidaGraph and a 1.5 ms dead time was added to all *x*-axis data points before fitting to obtain the corrected fluorescence amplitude. All fluorescence measurements were made in buffer containing 20 mM MOPS, pH 7.0, and 50 mM NaCl, at 25 °C. The free concentration of Mg^{2+} in the syringe containing the enzyme and in the cuvette of the stopped-flow instrument was always between 9.5 and 10 mM.

RESULTS

Steady-State Kinetics, Viscosometric, and Inhibition Studies. The steady-state kinetic parameters for phosphorylation of a synthetic peptide substrate, LRRASLG (Kemptide), by Acr-PKA have been previously measured (Lew et al., 1996) and are reported in Table 1. The steady-state kinetic parameters, k_{cat} and $K_{Kemptide}$, for Acr-PKA are less than 2-fold higher than those for wt-PKA, and K_{ATP} was 2.5-fold higher. The effects of increasing solvent viscosity on the steady-state kinetic parameters of Acr-PKA were measured and are expressed as the ratio of the observed parameter in the absence and the presence of added sucrose in Figure 1. Linear dependencies of both k_{cat} and $k_{cat}/K_{Kemptide}$ on relative solution viscosity were observed. The major effect of added viscosogen was on k_{cat} with only a minor effect on $k_{cat}/K_{Kemptide}$. The steady-state kinetic parameters and the slopes of their dependencies on solution viscosity are listed in Table 1 along with those previously measured for wt-PKA (Adams & Taylor, 1992; Lew et al., 1996). The inhibition constant for phosphokemptide was found to be 6.7 mM from initial velocity vs Kemptide double-reciprocal plots at varied, fixed concentrations of phosphokemptide (0−4 mM) and 1 mM ATP.

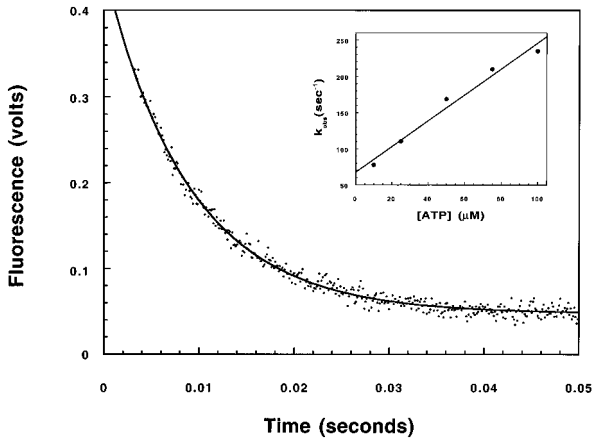

FIGURE 2: Time-dependent fluorescence change associated with the binding of ATP to Acr-PKA. Final concentrations of ATP and Acr-PKA are 25 and 0.18 μM, respectively. Data were corrected for a 1.5 ms instrument dead time and were fit to a single-exponential function to obtain an observed rate constant (k_{obs}) of 110 ± 5 s^{-1} for the reaction. The inset shows the dependence of k_{obs} on the concentration of ATP (10−100 μM).

Transient Kinetics. The rapid binding of nucleotides to the C-subunit of PKA was monitored by stopped-flow fluorescence spectroscopy. The binding of ATP and ADP were measured under pseudo-first-order reaction conditions ([ATP] or [ADP] ≫ [E]). The binding of both nucleotides causes a fluorescence quenching of the emission spectrum of the acrylodan label. A plot of fluorescence emission intensity (>420 nm) as a function of time is shown in Figure 2 for the binding of ATP (25 μM). A 1.5 ms dead time was added to the time data set. The time-dependent fluorescence change could be fit to a single-exponential function with a rate constant of 110 ± 5 s^{-1}. The data were interpreted according to a simple, one-step binding mechanism as shown in Scheme 1. The association and dissociation rate constants, k_{on} and k_{off}, were determined from plots of k_{obs} versus [ATP] or [ADP] according to

$$k_{obs} = k_{on}[L] + k_{off} \quad (2)$$

The observed rate constants for the binding of ATP are shown in the inset in Figure 2 under several nucleotide concentrations. A series of binding transients were also collected for ADP and plotted in similar fashion (data not shown). The values for the association and dissociation rate constants for ATP and ADP are summarized in Table 2.

To investigate whether nucleotide binding could be represented adequately by a simple one-step model (Scheme 1), we investigated the dependency of k_{obs} on ATP or ADP at high nucleotide concentrations. Fluorescence decay as a function of time required fitting with two exponentials at nucleotide concentrations greater than 50 μM. The biphasic time course for nucleotide binding was observed for both ATP and ADP. A typical recording at 200 μM ATP is

Table 2: Kinetic and Equilibrium Constants for Nucleotide Binding[a]

parameters	ATP	ADP
k_{on}[b] (μM^{-1} s^{-1})	1.8 ± 0.16	3.4 ± 0.17
k_{off}[c] (s^{-1})	68 ± 9.7	95 ± 4
k_{off} trap[d] (s^{-1})	61 ± 1.0	102 ± 1.0
k_{off}/k_{on}[e] (μM)	38 ± 6.4	28 ± 1.8
K_d[f] (μM)	25 ± 1.3	24 ± 1.3
k_f^{max} (s^{-1})	540 ± 20	580 ± 35
k_s^{av} (s^{-1})	48 ± 6	68 ± 17

[a] Experimental conditions as defined in Materials and Methods. [b,c] Determined by rapid binding/relaxation. [d] Determined by nucleotide competition as described in the legend to Figure 4. [e] Calculated from the ratio of *c*/*b*. [f] Determined by equilibrium titration.

Scheme 1

$$E \underset{k_{off}}{\overset{k_{on}[L]}{\rightleftharpoons}} E \bullet L$$

shown in Figure 3A. A 1.5 ms dead time was added to the time axis for data fitting. Fitting of the time-dependent fluorescence changes in Figure 3A to a double-exponential equation gave rate constants of 420 ± 10 s^{-1} and 40 ± 10 s^{-1} for the first (k_f) and the second (k_s) phases. For both nucleotides, k_f increased hyperbolically with nucleotide concentration, while k_s was concentration-independent (Figure 3B). Corrected amplitudes from eq 1 corresponding to the fast phase (ΔF_f) increased hyperbolically with nucleotide concentration up to 100 μM ATP but displayed a striking decrease in value at higher ATP concentrations, approaching a lower limit of ~50% maximum amplitude. The amplitudes corresponding to the slower phase (ΔF_s) were nucleotide-independent (Figure 3C). To ensure that the observed plateaus in both rate and amplitude reflect true ligand-independent phases, the binding experiment was repeated at 10 mM ATP. Under these conditions the transient was still biphasic and gave similar rate (k_f and k_s) and amplitude (ΔF_f and ΔF_s) fits as observed at 0.8 mM ATP (data not shown). Both the biphasic nature of the fluorescence quenching and amplitude dependence are similar for ADP binding (data not shown). The maximal values for k_f (k_f^{max}) and the average values for k_s (k_s^{av}) are presented in Table 2 for ATP and ADP.

The biphasic fluorescence decay at high nucleotide concentration was also observed under several buffer conditions of varying pH (pH 6.0−8.0) and ionic strength (50−500 mM NaCl) for both nucleotides (data not shown). Replacement of Mg^{2+} with Mn^{2+} gave similar biphasic kinetics at high ATP concentrations (data not shown). Fitting of the fluorescence quenching data under conditions of 10 mM $MnCl_2$ and 300 μM ATP gave values of 560 ± 55 s^{-1} and 12 ± 2 s^{-1} for k_f and k_s. Halving the concentration of ATP in the presence of the same amount of $MnCl_2$ gave similar rate fits to the fluorescence quenching data, indicating that this represents nucleotide-independent data (data not shown). Furthermore, similar biphasic kinetics were obtained with the binding of adenosine (data not shown). Fitting of the fluorescence quenching data under conditions of 10 mM $MgCl_2$ and 1000 μM adenosine gave values of 410 ± 33 s^{-1} and 27 ± 3 s^{-1} for k_f and k_s. Increasing the concentration of adenosine to 2.5 mM gave similar rates (data not shown).

Competition Experiments. The dissociation rate constants for ADP and ATP were also measured by a competition method. In this experiment, the enzyme and ligand are preequilibrated in one syringe in the stopped-flow instrument

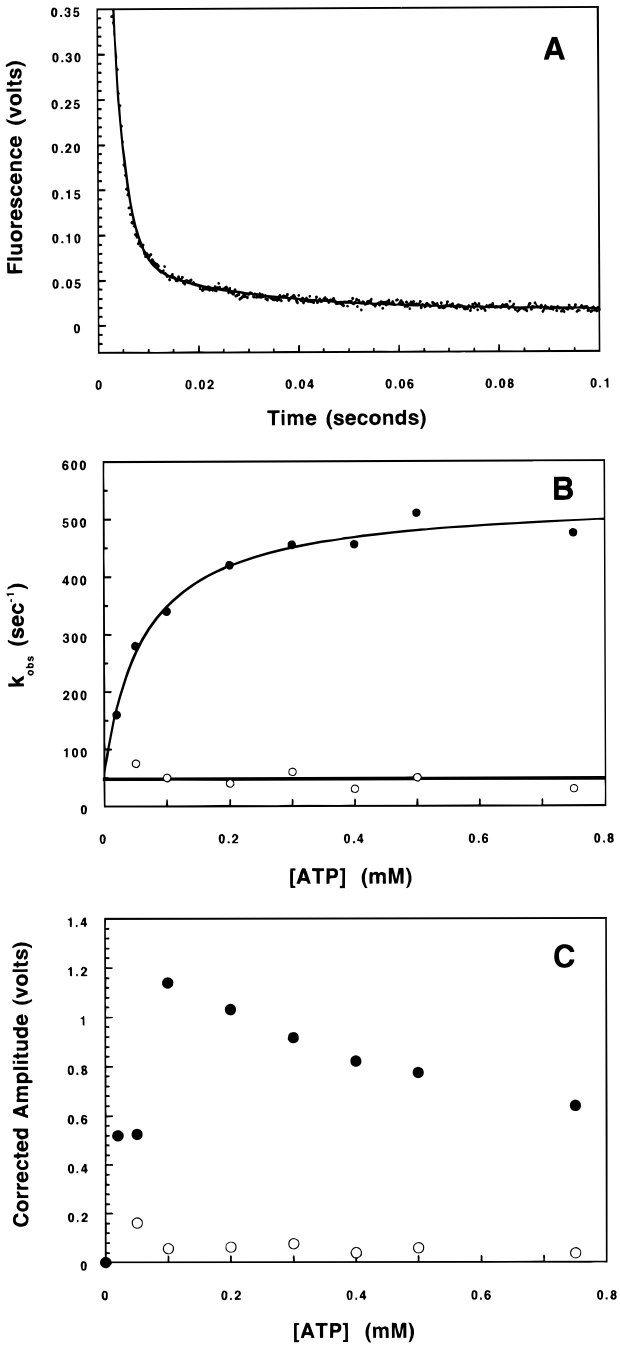

FIGURE 3: Time-dependent fluorescence change associated with the binding of ATP to Acr-PKA at various nucleotide concentrations. (A) Typical trace of fluorescence decay for the binding of ATP (200 μM). The data were fit to a double-exponential function to obtain rate constants of 420 ± 10 s^{-1} and 40 ± 10 s^{-1}. Dependence of the observed rate constants (B) and amplitudes (C) of the fast (●) and slow (○) phases, respectively, on ATP concentration. The upper limit for k_f is 540 ± 20 s^{-1} and the average value for k_s is 48 ± 6 s^{-1} (see Table 2).

Scheme 2

$$E \bullet L \underset{k_{on}[L]}{\overset{k_{off}}{\rightleftharpoons}} E + L$$
$$\downarrow [T]$$
$$E \bullet T$$

and rapidly mixed with large amounts of a trapping ligand in the other syringe. Since the fluorescence intensities of the respective ligand− and trap−enzyme complexes are different, the interconversion of these species can be monitored easily. The observed rate constant for the

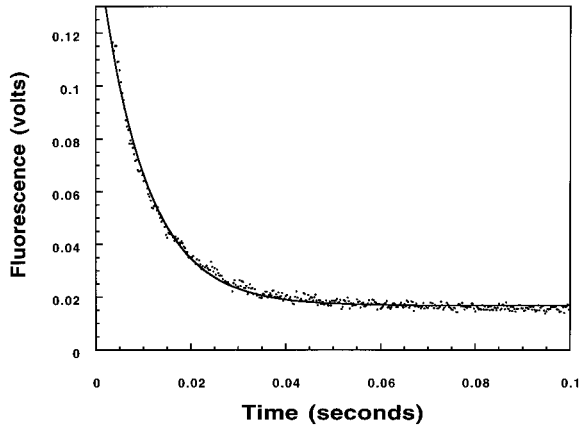

FIGURE 4: Dissociation rate constant for ADP determined by nucleotide trapping. Enzyme was preequilibrated with saturating concentrations (300 μM) of ADP and then rapidly mixed with an excess of ATP. An instrument dead time of 1.5 ms was added to the *x*-axis data set. Final concentrations of enzyme and ATP were 2.5 μM and 18 mM after mixing. The data were fit to a single-exponential function to obtain a rate constant of 102 $\pm$ 1.0 s^{-1}.

approach to equilibrium, k_{obs}, was measured by monitoring the time-dependent fluorescence change upon the displacement of one nucleotide for the other. This technique is demonstrated in the mechanism in Scheme 2, in which T is the trapping ligand and L is ATP or ADP. At high concentrations of T, the rate of conversion of E·L to E·T is limited by the dissociation rate constant, k_{off}. A typical competition experiment for the release of ADP is shown in Figure 4. The acrylodan fluorescence of the protein decreases as ATP displaces ADP since the former ligand better quenches the emission spectrum than the latter. The time-dependent fluorescence change was fit to a single-exponential function with a rate constant of 102 $\pm$ 1.0 s^{-1}. The observed rates of these transients were constant at all concentrations of the trapping agent between 6 and 24 mM, indicating that the rate of trapping is sufficiently large so that free enzyme and ligand cannot associate, and the observed rate constant for trap binding greatly exceeds k_{off}. Under these conditions, $k_{obs} = k_{off}$. The dissociation rate constants for ADP and ATP measured using this technique are listed in Table 2.

Pre-Steady-State Kinetics. Since the fluorescence emission properties of the E·ATP and E·ADP binary complexes are sufficiently different, the phosphorylation of the substrate peptide, Kemptide, could be monitored at the active site of the C-subunit. In this experiment, enzyme and ATP were preequilibrated in one syringe and then rapidly mixed with high concentrations of Kemptide in the other. The phosphorylation of the peptide was monitored as a time-dependent fluorescence increase. As shown in Figure 5, the observed transient is distinctly biphasic. The entire fluorescence change was complete in approximately 100 ms and no further changes in intensity were observed up to 10 s (data not shown). Under this enzyme concentration, a minimum of 5 s is required to phosphorylate 500 μM Kemptide, indicating that the transient monitors only the first turnover. The residuals for a single- and double-exponential fit to the data are also presented in Figure 5 and confirm that the transient is, indeed, biphasic. Fitting of the pre-steady-state transient to a double-exponential function gave rate constants of 550 $\pm$ 25 s^{-1} and 60 $\pm$ 30 s^{-1} for the fast (k_1) and the slow (k_2) phases. The observed amplitude for the fast phase (ΔF_1) was corrected for instrument dead time using eq 1. The total amplitudes for the pre-steady-state kinetic transients ($\Delta F_1 + \Delta F_2$) varied linearly with the total enzyme concentration, confirming that the observed burst phenomenon is not due to rapid product inhibition (data not shown).

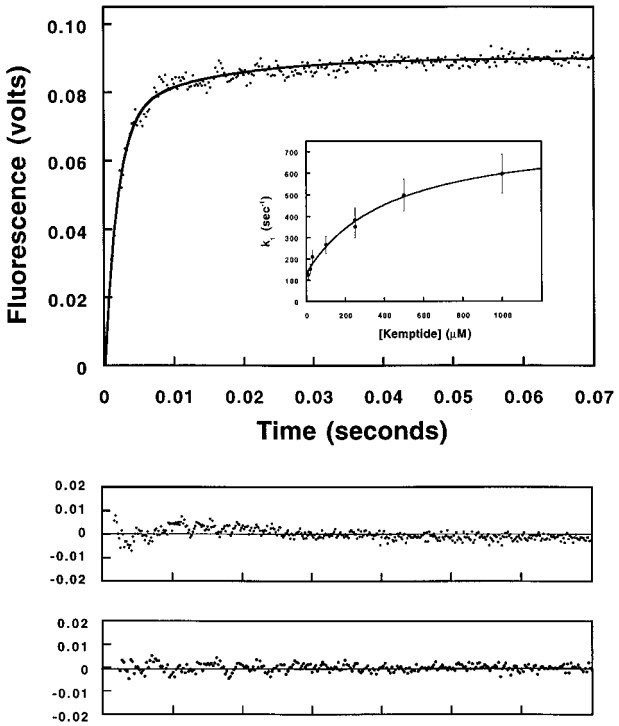

FIGURE 5: Pre-steady-state kinetic transient for Kemptide phosphorylation. Enzyme was preequilibrated with ATP and then rapidly mixed with Kemptide. Final concentrations were 2.5 μM enzyme, 1 mM ATP, and 500 μM Kemptide. The data were fit to a double-exponential function to obtain rate constants of 550 $\pm$ 25 s^{-1} and 60 $\pm$ 30 s^{-1} for the fast (k_1) and slow (k_2) phases. The residuals for single and double exponential fits are displayed in the middle and bottom panels. The inset to the upper panel shows the dependence of Kemptide concentration (10−1000 μM) on the observed rate constants for the fast phase. Hyperbolic fitting of the data provides maximum and minimum values of 650 $\pm$ 100 and 120 $\pm$ 20 s^{-1} for the fast phase, and the half-maximal rate occurs at a Kemptide concentration of 550 $\pm$ 25 μM.

Since it has been demonstrated previously using a rapid quench-flow technique that the burst phase is substrate-dependent, both k_1 and k_2 were monitored as a function of Kemptide concentration to obtain the upper limit for the burst rate constant. Although no substrate dependence is observed for k_2 (data not shown), k_1 varied hyperbolically with the concentration of Kemptide (Figure 5, inset). The data were fit to a hyperbolic function to obtain the concentration-independent value for k_1 (650 $\pm$ 100 s^{-1}). Extrapolation of the burst rate to zero Kemptide concentration gave a value of 120 $\pm$ 20 s^{-1}, and a half-maximal value for the upper and lower limits for k_1 occurred at a Kemptide concentration of 550 $\pm$ 25 μM. The pre-steady-state burst kinetics were also monitored in the presence of Mn^{2+}. A time-dependent fluorescence increase was observed that could be fit to a single exponential, whose rate constant was attenuated from 500 s^{-1} to 30 s^{-1} (Figure 6). Doubling the concentration of Kemptide from 500 to 1000 μM had no effect on the observed burst rate constant in the presence of Mn^{2+} (data not shown).

DISCUSSION

An important prerequisite for structure−function studies in protein kinases is a complete kinetic mechanism for substrate phosphorylation. While great strides have been

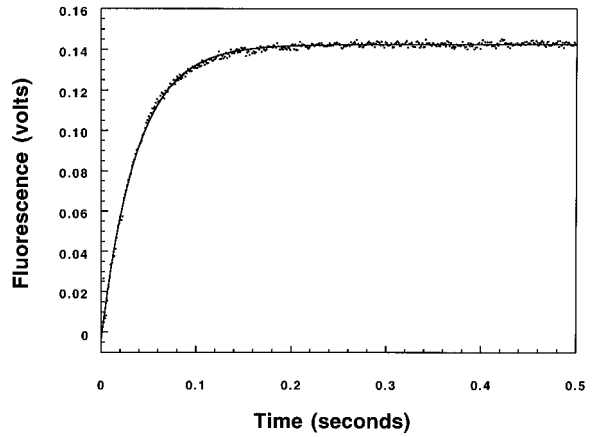

FIGURE 6: Pre-steady-state kinetic transient for Kemptide phosphorylation in the presence of $MnCl_2$. Conditions were identical to those described in the legend to Figure 5, except that $MgCl_2$ was replaced with an equivalent concentration (10 mM) of $MnCl_2$. Data were fit to a single-exponential function to obtain a rate constant of $30 \pm 1.5\ s^{-1}$.

made to understand the three-dimensional structure of protein kinases, a thorough comprehension of the individual steps associated with protein phosphorylation is pending. The paucity of detailed kinetic data for this group of catalysts stems from few biophysical probes for the enzymes. The kinetics of substrate and product binding has presented a problem owing to poor fluorescence properties. We have overcome this dilemma by constructing fluorescently labeled mutants of the C-subunit of PKA that are exquisitely sensitive to the binding of both ATP and ADP. In particular, one C-subunit mutant, acrylodan-labeled N326C, phosphorylates Kemptide with steady-state kinetic parameters that are similar to those for wild-type. The fluorescence emission spectrum of this mutant is quenched by the binding of either ATP or ADP. While the structural cause of this quenching is not precisely known, the presumption is that the binding of nucleotides induces conformational changes in the protein molecule that alter the local environment of the fluorophore, which is chemically attached to the C-terminal tail of PKA. However, this chemical attachment of the acrylodan label does not appear to perturb ATP or ADP binding. The thermodynamic dissociation constants of these two ligands have been measured previously (Lew et al., 1996) and found to be similar to those measured for the wild-type C-subunit by different techniques (Bhatnagar et al., 1983; Cook et al., 1982; Hoppe et al., 1978). In this paper we describe the kinetic nature of this ligand binding and offer evidence for partial rate limitation of k_{cat} by a nonchemical, unimolecular step.

The most detailed kinetic methods have shown that the phosphorylation of Kemptide by the C-subunit of PKA occurs by a simple three-step kinetic mechanism at high ATP concentrations. Viscosometric methods have demonstrated that k_{cat} is limited by a diffusion-controlled step which is presumed to be a product release step, namely, ADP dissociation (Adams & Taylor, 1992). Pre-steady-state kinetic analyses have shown that phosphoryl group transfer occurs in the active site at a rate constant that is more than 20-fold larger than k_{cat} (Grant & Adams, 1996). The rapid rate of phosphoryl transfer ($500\ s^{-1}$) and slow release of products ($20\ s^{-1}$) then explain why the K_m for Kemptide is more than 10-fold lower than its K_d value despite it being in rapid equilibrium with the active site. The simple kinetic mechanism for PKA involving slow release of ADP hinges upon the presumption that any unimolecular reactions associated with catalysis excluding the chemical step (i.e., phosphoryl transfer) are not sensitive to solvent viscosity. We demonstrate in this paper that a conformational change in a fluorescently labeled mutant of PKA partially controls maximum turnover. The viscosity dependence of this added step implies that it involves significant structural movement within the protein.

Steady-State Kinetics and Viscosometric Studies. The goal of this kinetic study was to gather insight into the kinetic mechanism of protein phosphorylation catalyzed by the wild-type C-subunit of PKA. The objective of these studies presented in this paper is to use a mutant C-subunit for understanding the wild-type protein. The effects of mutation on both the steady-state kinetic parameters and the viscosity sensitivity of these parameters suggest that our assumption is, indeed, valid. The effects of mutation and fluorescent labeling on the steady-state kinetic parameters for Kemptide phosphorylation have been reported and compared to the wild-type enzyme previously (Lew et al., 1996). As summarized in Table 1, no significant changes in the steady-state kinetic parameters are found compared to the wild-type enzyme. In fact, the largest difference is in the 2.5-fold increase in K_{ATP}, while k_{cat} and $K_{Kemptide}$ for the enzyme are perturbed less than or equal to 1.5-fold (Table 1). We now report a full viscosity effect on k_{cat} [$(k_{cat})^{\eta} \approx 1$] that is fully consistent with the wild-type enzyme (Table 1) and supports the validity of our comparison. A small viscosity effect is measured on $k_{cat}/K_{Kemptide}$ (Table 1) and is consistent with a faster release of Kemptide compared to phosphoryl transfer. The observed value for $(k_{cat}/K_{Kemptide})^{\eta}$ can be used to determine an association rate constant of $7.2 \pm 2.3\ \mu M^{-1}\ s^{-1}$ for Kemptide.[2] These data are consistent with a kinetic mechanism in which the substrate is in rapid equilibrium with the active site and maximum turnover is controlled by a diffusion event, namely, ADP release, as previously demonstrated for the wild-type C-subunit (Adams & Taylor, 1992). Although this information is valuable, it does not tell us whether ADP or phosphopeptide release controls turnover or whether viscosity-dependent conformational changes are important for this parameter.

Nucleotide Binding Studies. We used stopped-flow kinetic techniques to characterize the transient association and dissociation of both ATP and ADP. The observed rate constants are shown in Table 2 and are corroborated by two independent techniques. The dissociation rate constants were determined by (1) relaxation (Figure 3) and (2) competition (Figure 4) methods, both of which resulted in similar values. Furthermore, the ratio of the observed dissociation and association rate constants (k_{off}/k_{on}) of both nucleotides were similar to their K_d values determined by equilibrium fluorescence quenching (Table 2). These data are consistent with a simple, one-step binding pathway as shown in Scheme 1 for both nucleotides and support an alternative interpretation of the viscosity results. The kinetic nucleotide binding data demonstrate that the observed ADP dissociation rate constant is approximately 2.5-fold higher than the steady-state rate constant for maximum turnover (k_{cat}), providing evidence that

[2] The association (k_2) and dissociation (k_{-2}) rate constants for Kemptide can be evaluated according to the two following relationships: $k_2 = k_{cat}/K_{Kemptide}/(k_{cat}/K_{Kemptide})^{\eta}$ and $k_{-2} = k_3\ [1 - (k_{cat}/K_{Kemptide})^{\eta}]/(k_{cat}/K_{Kemptide})^{\eta}$, where k_3 is the phosphoryl transfer rate constant (Adams & Taylor, 1992).

another step in the internal catalytic mechanism must be partially rate-determining. If this is so, the maximum rate constant for catalysis must be limited partially by this other step and this step, by definition, must be sensitive to solvent viscosity. We will demonstrate in the next section that phosphokemptide release cannot account for the observed turnover number.

The association rate constant for ATP measured by relaxation binding is similar in value to k_{cat}/K_m for ATP (Tables 1 and 2), suggesting that the rate-determining step for the enzyme reaction under limiting ATP concentrations is nucleotide association. This assertion is validated by two independent studies. First, Kong and Cook (1988) demonstrated that 100% of [γ-^{32}P] ATP is trapped as radioactive phosphokemptide at all concentrations of free Mg^{2+}. This indicates that ATP dissociates from the ternary substrate complex, E·ATP·Kemptide, at a rate constant that is much lower than that for the catalytic steps. Second, Adams and Taylor (1992) have shown through viscosometric techniques that k_{cat}/K_m for ATP is diffusion-controlled, indicating that the rate constant for phosphoryl group transfer greatly exceeds that for ATP release.

The binding of a small ligand to a protein molecule is, in most cases, inadequately represented by a simple one-step model. Rather, the initial encounter of a ligand with its receptor is commonly accompanied by one or more conformational changes (Gutfreund, 1995). Indeed, the detection of two nucleotide-independent phases in the relaxation experiment (Figure 3B) shows that conformational events are associated with ligand binding in PKA. We interpret the hyperbolic dependence of k_f with respect to nucleotide concentration and the nucleotide independence of k_s to depict a mechanism whereby ATP and ADP binding must comprise at least three steps: a ligand-dependent, bimolecular step and two conformational steps which are ligand-independent at high ATP/ADP concentrations (>400 μM). The nonhyperbolic dependence of the amplitude of the fast phase (Figure 3C) indicates that formation of the initial encounter is not faster than the other two steps at low nucleotide concentrations. We propose that at low concentrations the binding of nucleotide is sufficiently slow that the observed rate (k_f) represents a mixture of this step and associated conformational changes. At high nucleotide concentrations (>100 μM), this step is progressively lost in the dead time of the instrument. The corresponding decrease in amplitude with increasing nucleotide levels (Figure 3C) suggests that a significant fluorescence amplitude is associated with this initial ligand-binding step. The observation of two ligand-independent phases of similar magnitude for the binding of adenosine and Mn·ATP indicates that these conformational changes are not linked to the triphosphate binding region of the active site. Likewise, these similarities in rate imply that the fast phase in the pre-steady-state transient (Figure 5) is not associated with a conformational change forced by the nucleotide.

Pre-Steady-State Kinetic Studies. Pre-steady-state kinetic techniques are perhaps the most informative for analyzing individual steps in an enzymatic reaction. For example, rapid quench-flow techniques have been used to demonstrate that the C-subunit of PKA phosphorylates Kemptide with a rate constant that is 25-fold larger than k_{cat} (Grant & Adams, 1996). This rapid rate of phosphoryl group transfer (500 s^{-1}) in the active site then explains the high catalytic efficiency of this enzyme (i.e., k_{cat}/K_m) and the 100-fold lower

Scheme 3

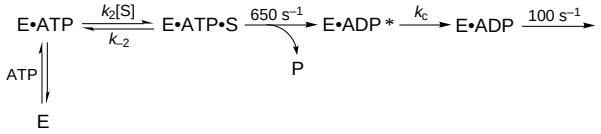

K_m for Kemptide compared to K_d. We took advantage of the differential fluorescence quenching of ATP and ADP to monitor the phosphoryl transfer step in the labeled mutant. Surprisingly, we found that the pre-steady-state kinetic burst phase for the labeled enzyme is composed of two distinct, exponential phases rather than one (Figure 5). The rate constant for the first phase (k_1) varied hyperbolically with the Kemptide concentration (Figure 5, inset). This has been observed previously in rapid quench-flow studies and is consistent with equilibrium binding of the substrate prior to phosphoryl transfer (Grant & Adams, 1996). For a simple three-step mechanism (substrate binding, phosphoryl transfer, and net product release), the extrapolation of the burst rate to infinite substrate concentration gives the true phosphoryl transfer rate constant and the extrapolation to zero substrate concentration gives the net rate constant for product release. The concentration at which an intermediate rate is observed provides the true dissociation constant for Kemptide. Although the values obtained from the fitting of k_1 in Figure 5 (inset) is consistent with previous reports on the kinetic mechanism, we are cautious not to overinterpret these results since an additional step is now present in the mechanism. Given this caveat, we use only the extrapolated rate at infinite substrate concentration to provide the true burst rate constant (650 s^{-1}). The reduction in the observed burst rate constant of 20-fold upon Mn^{2+} substitution (Figure 6) suggests that this initial phase represents the true phosphoryl transfer step rather than a conformational change. However, the possibility that this initial phase represents a cation-dependent step preceding a faster phosphoryl transfer step cannot be formally ruled out.

Since the rate constant for phosphoryl group transfer is approximately 12-fold larger than maximum turnover, the chemical step has little influence on the value of this parameter. We propose that the second phase observed in the pre-steady-state kinetics (60 s^{-1}) is the source of the lower value for k_{cat}. We presume that the release rate of phosphokemptide does not influence either the maximum turnover rate or this second phase. This assumption is based on two results. First, the measured K_i value for phosphokemptide toward Acr-PKA is 6.7 mM, a value that is approximately 10-fold greater than the K_d for Kemptide based on K_i measurements for the Ala-Kemptide analog inhibitor (Lew et al., 1996). Second, a minimal viscosity effect on $k_{cat}/K_{Kemptide}$ for PKA (Table 1) implies that the rate constant for Kemptide dissociation is significantly larger than the rate of phosphoryl transfer. These two observations imply that the dissociation rate constant for phosphokemptide must be exceedingly large relative to that for ADP release and maximum turnover. A K_i value of 6.7 mM places a dissociation rate constant for phosphokemptide of 47 000 s^{-1}, assuming an association rate constant similar to that of Kemptide , 7 μM^{-1} s^{-1}, determined from viscosometric studies (Table 1 and footnote 2).

A simple catalytic mechanism which is consistent with the nucleotide binding, trapping, and pre-steady-state kinetic data is shown in Scheme 3, where S represents Kemptide,

k_2 and k_{-2} are the association and dissociation rate constants for Kemptide, and k_c is the rate constant for the conformational change. In this mechanism, phosphoryl transfer and phosphokemptide release are fast and the final release of ADP occurs in two distinct steps. We presume that this is not a unique solution for all the data for several reasons. First, we are unclear whether the free enzyme exists in one or more conformers. Second, we do not know whether the binary nucleotide−enzyme complex, E·ADP*, can dissociate the nucleotide followed by free enzyme isomerization (E* → E), creating a bifurcated pathway for product release. Third, we assume in this mechanism that the second phase in the pre-steady-state represents a favorable step ($k_c > k_{-c}$), a simplification that permits us to assign an individual rate constant to this step. If there were a significant reverse component to this step that was comparable in rate to the dissociation rate constant for ADP or other conformational change steps, then the observed rate of 60 s^{-1} (Figure 5) would represent a composite value of several individual rate constants. Also, we cannot conclude definitively that there is any more than a coincidental relationship between the values of k_s for ADP binding (Table 2) and k_2 for the pre-steady-state kinetic transient (Figure 5) since neither observed phase may represent a discrete step in the mechanism. Since the relaxation and pre-steady-state kinetic studies are irresolute on these issues, there are a number of possible scenarios that can explain the three-step binding data for nucleotides and the biphasic pre-steady-state kinetics. The salient point in this data, however, is that there are conformational changes associated with nucleotide binding and catalytic turnover that may represent similar conformational events important for catalysis, and the mechanism in Scheme 3 depicts a likely sequence for catalytic cycling.

Structural Dynamics. Since the first crystallographic observations of enzyme conformational changes in hexokinase, it has become apparent that protein structural changes are important for both substrate/product binding and catalysis. For the C-subunit of PKA, there are several reports of conformational changes associated with ligand binding. Perhaps the most detailed reports stem from X-ray crystallography and low-angle neutron scattering. The three-dimensional structures of several crystal forms of the C-subunit of PKA have been successfully solved and reveal unique properties of the enzyme. The C-subunit is composed of two domains—a large substrate binding subdomain and a small nucleotide binding subdomain. Two distinct structures have been crystallized: one in an open and the other in a closed conformation (Zheng et al., 1993b). These two structures differ by only the relative orientation of the two subdomains. It is presumed, based on the basis of the orientation of the active-site residues, that the open conformation is inactive and the closed conformation is active. Solution X-ray scattering was used to measure the radii of these two forms and suggested that inhibitor binding induces the closed form (Olah et al., 1993). Although it is evident that both forms exist in solution and in the crystal form, it is unclear from the preceding reports whether these forms have any kinetic relevance under normal catalytic cycling.

The observation of a second phase in the pre-steady-state, stopped-flow kinetic studies implies that a structural change occurs under normal catalytic cycling for this mutant. Furthermore, the dependence of k_{cat} on solvent viscosity suggests that this conformational change must be large enough so that the intramolecular movement of the protein is impeded by the solvent. Given the substantial evidence that the C-subunit can adopt open and closed forms that would be expected to reorganize the solvent layer on the protein surface, subdomain movements may influence catalysis in this mutant by lowering the value of k_{cat}. Alternatively, the conformational event may represent a distinct movement(s) that is required for substrate turnover. Since this labeled mutant is kinetically similar to the wild-type enzyme, we propose that this conformational change may have kinetic significance for normal substrate turnover. Given this proposal, the data presented in this paper are the first linkage between a structural change and catalysis in a protein kinase.

REFERENCES

Adams, J. A., & Taylor, S. S. (1992) *Biochemistry 31*, 8516−8522.

Bhatnagar, D., Roskoski, R. J., Rosendahl, M. S., & Leonard, N. J. (1983) *Biochemistry 22*, 6310−6317.

Cook, P. F., Neville, M. E., Vrana, K. E., Hartl, F. T., & Roskoski, J., R. (1982) *Biochemistry 21*, 5794−5799.

DeBont, H. L., Rosenblatt, J., Jancarik, J., Jones, H. D., Morgan, D. O., & Kim, S. H. (1993) *Nature 363*, 595−602.

Frank, D. A., & Greenberg, M. E. (1994) *Cell 79*, 5−8.

Grant, B., & Adams, J. A. (1996) *Biochemistry 35*, 2022−2029.

Grieco, B. D., Porcellini, A., Avvedimento, E. V., & Gottesman, M. E. (1996) *Science 271*, 1718−1723.

Hanks, S. K., & Hunter, T. (1995) *FASEB J. 9*, 576−596.

Hoppe, J., Freist, W., Marutzky, R., & Shaltiel, S. (1978) *Eur. J. Biochem. 90*, 427−432.

Jeffrey, P. D., Russo, A. A., Polyak, K., Gibbs, E., Hurwitz, J., Massague, J., & Pavletich, N. P. (1995) *Nature 376*, 313−320.

Kong, C.-T., & Cook, P. F. (1988) *Biochemistry 27*, 4795−4799.

Lew, J., Tsigelny, I., Coruh, N., Garrod, S., & Taylor, S. S. (1996) *J. Biol. Chem. 272*, 1507−1513.

Madhusudan, Trafny, E. A., Xuong, N.-h., Adams, J. A., Ten Eyck, L. F., Taylor, S. S., & Sowadski, J. M. (1994) *Protein Sci. 3*, 176−187.

Montminy, M. R., Gonzalez, G. A., & Yamamoto, K. K. (1990) *Trends Neurosci. 13*, 184−188.

Olah, G. A., Mitchell, R. D., Sosnick, T. R., Walsh, D. A., & Trewhella, J. (1993) *Biochemistry 32*, 3649−3657.

Qamar, R., Yoon, M.-Y., & Cook, P. F. (1992) *Biochemistry 31*, 9986−9992.

Taylor, S. S., & Radzio-Andzelm (1994) *Structure 2*, 345−355.

Taylor, S. S., Buechler, J. A., & Knighton, D. R. (1990) in *Peptides and Protein Phosphorylation* (Kemp, B. E., Ed.) pp 1−42, CRC Press, Inc., Boca Raton, FL.

Walsh, D. A., Perkins, J. P., & Krebs, E. G. (1968) *J. Biol. Chem. 243*, 3763−3765.

Whitehouse, S., & Walsh, D. A. (1983) *J. Biol. Chem. 258*, 3682−3692.

Whitehouse, S., Feramisco, J. R., Casnellie, J. E., Krebs, E. G., & Walsh, D. A. (1983) *J. Biol. Chem. 258*, 3693−3701.

Zheng, J., Knighton, D. R., Ten Eyck, L. F., Karlsson, R., Xuong, N.-h., Taylor, S. S., & Sowadski, J. M. (1993a) *Biochemistry 32*, 2154−2161.

Zheng, J., Knighton, D. R., Xuong, N.-h., Taylor, S. S., Sowadski, J. M., & Ten Eyck, L. F. (1993b) *Protein Sci. 2*, 1559−1573.

BI963164U